NASA/TM—2008-215162

A Stereo Imaging Velocimetry Technique for Analyzing Structure of Flame Balls at Low Lewis-Number (SOFBALL) Data

Mark McDowell
Glenn Research Center, Cleveland, Ohio

Elizabeth Gray
Scientific Consulting, Inc., Cleveland, Ohio

April 2008

NASA STI Program . . . in Profile

Since its founding, NASA has been dedicated to the advancement of aeronautics and space science. The NASA Scientific and Technical Information (STI) program plays a key part in helping NASA maintain this important role.

The NASA STI Program operates under the auspices of the Agency Chief Information Officer. It collects, organizes, provides for archiving, and disseminates NASA's STI. The NASA STI program provides access to the NASA Aeronautics and Space Database and its public interface, the NASA Technical Reports Server, thus providing one of the largest collections of aeronautical and space science STI in the world. Results are published in both non-NASA channels and by NASA in the NASA STI Report Series, which includes the following report types:

- TECHNICAL PUBLICATION. Reports of completed research or a major significant phase of research that present the results of NASA programs and include extensive data or theoretical analysis. Includes compilations of significant scientific and technical data and information deemed to be of continuing reference value. NASA counterpart of peer-reviewed formal professional papers but has less stringent limitations on manuscript length and extent of graphic presentations.

- TECHNICAL MEMORANDUM. Scientific and technical findings that are preliminary or of specialized interest, e.g., quick release reports, working papers, and bibliographies that contain minimal annotation. Does not contain extensive analysis.

- CONTRACTOR REPORT. Scientific and technical findings by NASA-sponsored contractors and grantees.

- CONFERENCE PUBLICATION. Collected papers from scientific and technical conferences, symposia, seminars, or other meetings sponsored or cosponsored by NASA.

- SPECIAL PUBLICATION. Scientific, technical, or historical information from NASA programs, projects, and missions, often concerned with subjects having substantial public interest.

- TECHNICAL TRANSLATION. English-language translations of foreign scientific and technical material pertinent to NASA's mission.

Specialized services also include creating custom thesauri, building customized databases, organizing and publishing research results.

For more information about the NASA STI program, see the following:

- Access the NASA STI program home page at *http://www.sti.nasa.gov*

- E-mail your question via the Internet to *help@sti.nasa.gov*

- Fax your question to the NASA STI Help Desk at 301–621–0134

- Telephone the NASA STI Help Desk at 301–621–0390

- Write to:
  NASA Center for AeroSpace Information (CASI)
  7115 Standard Drive
  Hanover, MD 21076–1320

NASA/TM—2008-215162

A Stereo Imaging Velocimetry Technique for Analyzing Structure of Flame Balls at Low Lewis-Number (SOFBALL) Data

Mark McDowell
Glenn Research Center, Cleveland, Ohio

Elizabeth Gray
Scientific Consulting, Inc., Cleveland, Ohio

National Aeronautics and
Space Administration

Glenn Research Center
Cleveland, Ohio 44135

April 2008

This work was sponsored by the Fundamental Aeronautics Program
at the NASA Glenn Research Center.

Level of Review: This material has been technically reviewed by technical management.

Available from

NASA Center for Aerospace Information
7115 Standard Drive
Hanover, MD 21076–1320

National Technical Information Service
5285 Port Royal Road
Springfield, VA 22161

Available electronically at http://gltrs.grc.nasa.gov

A Stereo Imaging Velocimetry Technique for Analyzing Structure of Flame Balls at Low Lewis-Number (SOFBALL) Data

Mark McDowell
National Aeronautics and Space Administration
Glenn Research Center
Cleveland, Ohio 44135

Elizabeth Gray
Scientific Consulting, Inc.
Cleveland, Ohio 44135

Abstract

Stereo Imaging Velocimetry (SIV) is a NASA Glenn Research Center (GRC) developed fluid physics technique for measuring three-dimensional velocities in any optically transparent fluid that can be seeded with tracer particles. SIV provides a means to measure three-dimensional fluid velocities quantitatively and qualitatively at many points. This technique provides full-field 3–D analysis of any optically clear fluid or gas experiment using standard off-the-shelf CCD cameras to provide accurate and reproducible 3–D velocity profiles for experiments that require 3–D analysis. A flame ball is a steady flame in a premixed combustible atmosphere which, due to the transport properties (low Lewis-number) of the mixture, does not propagate but is instead supplied by diffusive transport of the reactants, forming a premixed flame. This flame geometry presents a unique environment for testing combustion theory. We present our analysis of flame ball phenomena utilizing SIV technology in order to accurately calculate the 3–D position of a flame ball(s) during an experiment, which can be used as a direct comparison of numerical simulations.

Introduction

Stereo Imaging Velocimetry (SIV) is a technique for obtaining quantitative, 3–D flow information from any transparent liquid, gas or air experiment seeded with tracer particles. SIV provides a non-intrusive means for measuring 3–D fluid velocities at many points and is the world's first 3–D full-field quantitative and qualitative diagnostic tool (Bethea, 1996). It was developed for use for NASA's Microgravity science experiments as well as industrial applications. The components of a typical SIV system include: 2–D or 3–D camera calibration, centroid determination with particle overlap decomposition, particle tracking, stereo matching, and 3–D velocity analysis.

An SIV compatible experiment consists of at least two CCD cameras, oriented at 90° with respect to each other (orthogonal), observing an experiment volume that has been seeded with neutrally buoyant tracer particles that are imaged as the experiment is run. Each camera records two-dimensional data of the motion of the tracer particles in the observation volume and three-dimensional data is obtained by computationally combining the two-dimensional information (McDowell and Gray, 2004).

The objective of this technical memorandum is to provide a technique to calculate the 3–D positions of the Structure of Flame Balls at Low Lewis-number (SOFBALL) experiment flown on STS–107. The goal is to study the behavior and properties of a newly discovered premixed-gas flame phenomena called flame balls. These spherical, stable, stationary flame structures, observed only in microgravity, provide the opportunity to study the interactions of the two most important processes necessary for combustion (chemical reaction and heat/mass transport) in the simplest possible configuration. SOFBALL experiments were conducted by filling a 26-liter chamber with a weakly combustible gas (hydrogen or methane and oxygen highly diluted with an inert gas) and igniting the mixture with a spark. The flames were imaged using two black and white video cameras and one color camera. No seeding particles were used in the experiments since the phenomena we were tracking with our SIV system were flameballs and

not particles. The two black and white cameras were positioned orthogonally to each other. Radiometers, thermocouples and pressure transducers were used to determine the heat release from the flame balls. The experiments were performed in the Combustion Module-2 facility on the STS-107 SPACEHAB mission. What follows is a description of our SIV technique applied to SOFBALL data.

SIV Background

An in-depth explanation of each phase of SIV can be found (McDowell and Gray, 2004) and (Bethea, 1996) in order to give the reader a better understanding of SIV. A brief description of each of the phases of a typical SIV experiment is needed before explaining how our SIV technique was applied to SOFBALL experimental data.

Three–Dimensional Camera Calibration

Prior to running an SIV experiment, the observation volume must be calibrated in order to get a 2–D to 3–D mapping of the experiment. Three-dimensional camera calibration is a process by which one determines the geometrical and experimental parameters for a particular experimental chamber and imaging system. The geometrical parameters are the internal camera characteristics such as focal length and pixel size. The experimental parameters are the orientation of the cameras and chamber relative to a world coordinate system, the refractive characteristics of the system, and any lens aberrations or distortions present in the cameras. Camera calibration is the most important aspect of any machine vision experiment since it serves as a lower limit for determining system accuracy and permits us to make the jump from qualitative to quantitative data. The nomenclature of the SIV 3–D camera calibration is shown in figure 1. Following the steps outlined by (Bethea, 1996) and (Bethea, et al, 1997), one can determine the camera calibration error associated with a typical SIV experiment.

Centroid Determination

In order to accurately identify individual objects or particles in an image, it is necessary to perform standard image preprocessing techniques such as threshold that separate the objects from the background. Once this is completed, the intensity-weighted center of mass of each object is identified and labeled by using a technique described by (McDowell, 2004). A probabilistic feature mapping predicting the probability that an object region is a single, double, and triple particle is obtained following the extraction of the feature vector (major axis length, circumference). This is accomplished by entering the features into the empirically derived probability equations in figure 2, where x is the value of the feature.

Particle tracking is used to determine the motion of objects or particles in either two or three dimensions by measuring the incremental distances moved by each particle between each frame. The success of any particle tracking technique depends on how heavily the flow is seeded, the frame rate of the image acquisition hardware, and the velocity of the particles. Using information about the maximum expected velocity, we link particle identities through four frame sequences, establishing their paths of motion in the process. Our particle tracking technique uses an adaptive guided evolutionary neural net with simulated annealing to arrive at a globally optimal assignment of tracks where the neural net is ‘guided’ both by the minimization of the search space through the use of limiting assumptions about valid tracks and by a strategy which seeks to avoid high-energy intermediate states by eliminating overlapping tracks that can trap the neural net in a local minimum (McDowell and Gray, 2004) and (Crouser et al., 1995). Figures 3 and 4 give a general description of how we determine a valid track pattern.

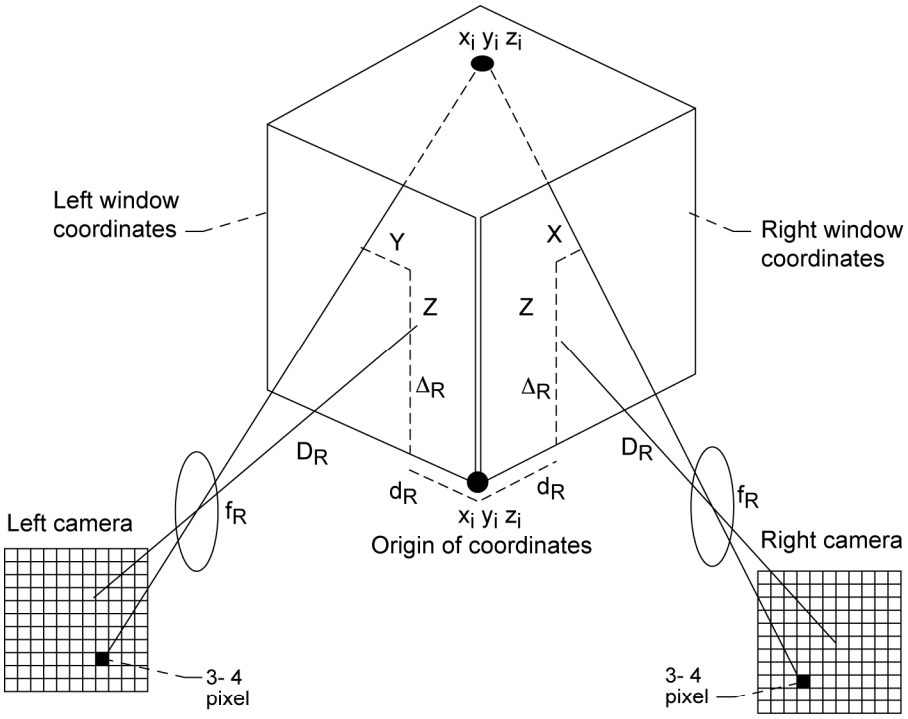

$x_i\ y_i\ z_i$ = Absolute x y z coordinates of particle i.
$X_R^i\ Z_R^i$ = Window coordinates of particle i on the right face of the chamber.
$x_R^i\ z_R^i$ = Pixel coordinates of particle i as seen by the right camera.
f_R = Focal length of the right camera.
D_R = Distance between the right camera and the face of the chamber.
d_R = Horizontal distance of the right camera axis from the origin.
Δ_R = Vertical distance of the right camera axis from the origin.
C_R = Camera dependent constant with the units mm/pixel.

Figure 1.—Camera calibration nomenclature, right camera perspective (left camera is analogous).

$$P(single) = 1 - \frac{1}{1 - e^{-\frac{x+q}{t}}} \qquad P(triple) = 1 - \frac{1}{1 - e^{-\frac{x+b}{c}}} \qquad P(double) = 1 - P(single) - P(triple)$$

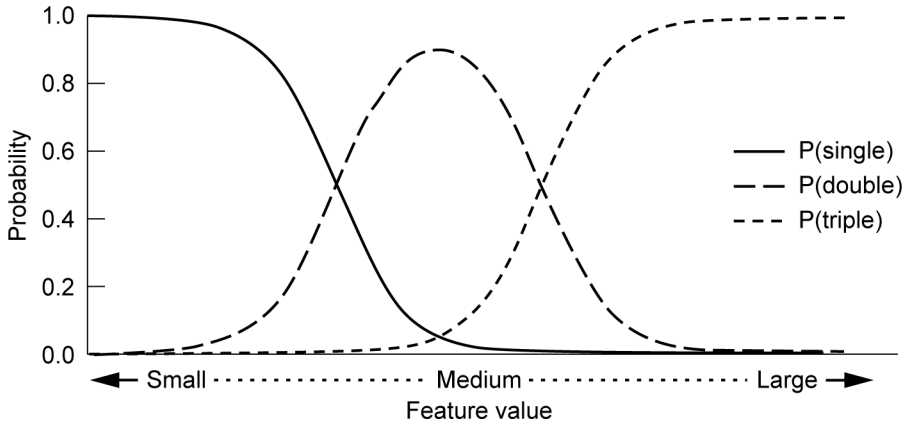

Figure 2.—Probability relationships for a single, double and triple object.

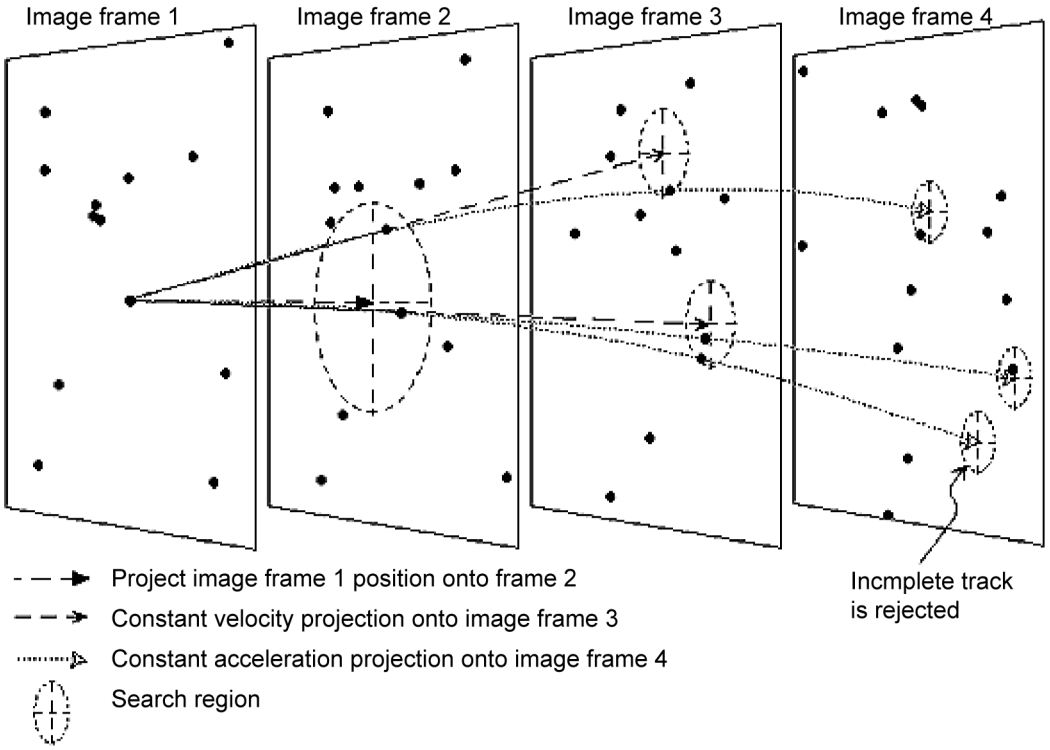

Figure 3.—Schematic illustration of how potentially valid tracks are identified. An empty search region terminates a track fragment. In this example, two valid tracks are identified for the original particle. The process is continued until only the valid track remains.

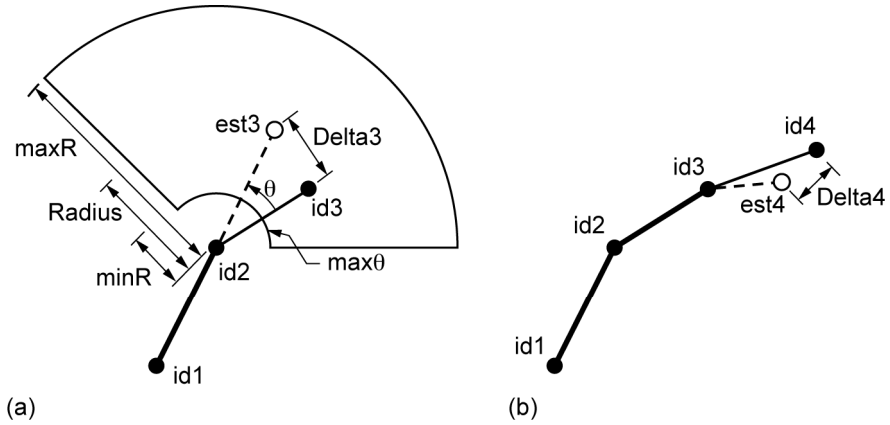

Figure 4.—Track errors. Delta3 measures the difference between the actual and estimated position (based on an assumption of zero acceleration) of a particle in frame 3. Delta4 measures the difference between the actual and estimated position (based on an assumption of constant acceleration) of a particle in frame 4. (a) Track straightness error. (b) Track smoothness error.

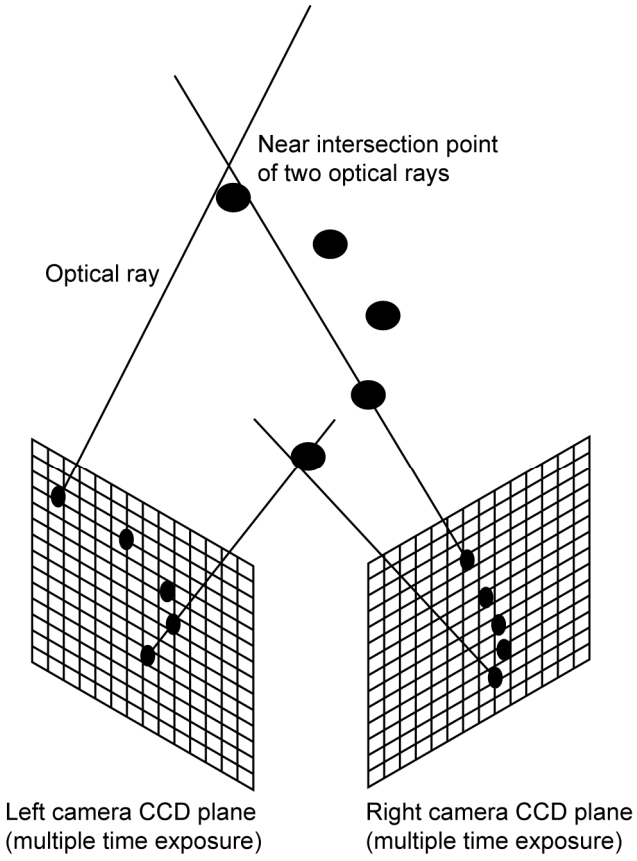

Figure 5.—Stereo matching of a track that appears in the right and left orthogonal camera views.

Stereo Matching

Stereo matching determines which of the many particle tracks in a pair of synched images from two cameras represent the same particle track imaged from different camera perspectives. Given two sets of 2–D tracks, one set from each of two orthogonal views, our stereo-matching module provides the ability to stereo-match the tracks and determine a globally optimal solution (McDowell and Gray, 2004). Figure 5 shows a graphical representation of our stereo matching technique where optimization error is taken to be the sum of the squared vertical displacements (in pixels) between corresponding particle images, on a frame-by-frame basis, matching a given track from the left view with one in the right view. This is similar to the approach taken in (Trigui et al., 1992).

Methods and Materials

We have applied our SIV techniques to the problem of calculating the 3–D positions of the Structure of Flame Balls at Low Lewis-number (SOFBALL) experimental data. What follows is a description as well as examples of how SIV was utilized to study the behavior and properties of a newly discovered premixed-gas flame phenomena called flame balls.

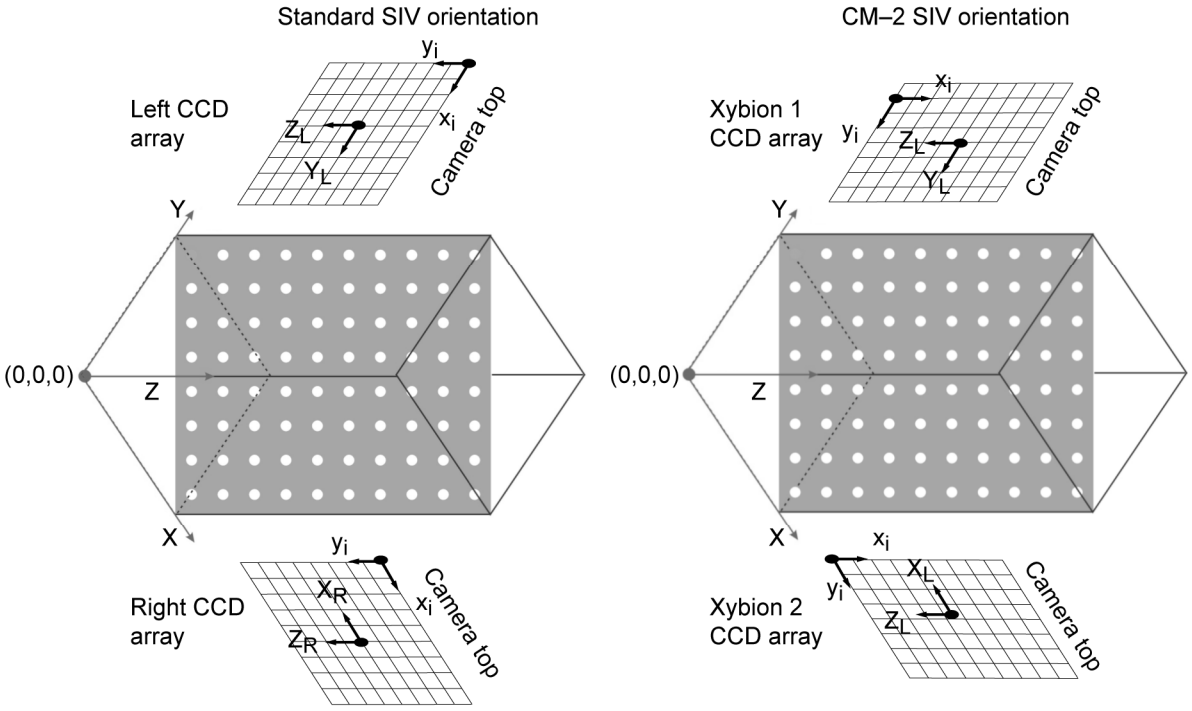

Figure 6.—SOFBALL camera orientation compared to standard SIV orientation. X, Y, Z: absolute coordinates. x_i, y_i: image coordinates. X_R, Z_R, Y_L, Z_L: window coordinates for right and left views.

Experimental Chamber

The SOFBALL camera CCD arrays are rotated 90° with respect to the camera bodies (figure 6). The experimental chamber was cylindrical and about 62 cm long and 40 cm in diameter. This meant that a customized calibration technique needed to be developed and incorporated into the analysis in order to verify the accuracy of our technique.

Calibration Target Grid

A calibration target grid needs to be constructed and analyzed in order for us to calculate experimental errors such as pixel quantization errors and a valid 2–D to 3–D mapping function. The parameters used for the calibration grid are shown in figure 7.

The grid pattern shown in figure 7 was used in order to place calibration grid that would accuracy calibrate the chamber. Since the chamber is approximately 19 cm long, we chose to place a calibration grid at the front, center and back of the chamber representing +8 cm, 0 cm and –8 cm, respectively. The optimal set of points was determined to be 80 points from the center plane combined with 20 points each from the +8.0 cm plane and the –8.0 cm plane as shown in figure 8.

For each set of calibration coefficients, we used the left and right view coordinates of the test points and the calibration coefficients to determine the predicted 3–D coordinates of the test points. This allowed us to mathematically convert the 2–D grid coordinates into 3–D absolute coordinates. This conversion is shown in figure 9.

10 rows, 8 columns
(illuminated dots on a black background,
inversion of bigGrid.cdr)
H: 228.6 mm
W: 177.8 mm
Particle diameter: 4.0 mm
x_0 = 0.0 mm
y_0 = 0.0 mm
Δ_x = 25.4 mm
Δ_y = 25.4 mm

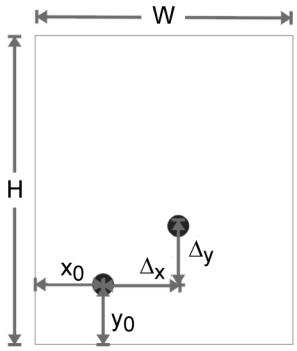

Figure 7.—Calibration target grid.

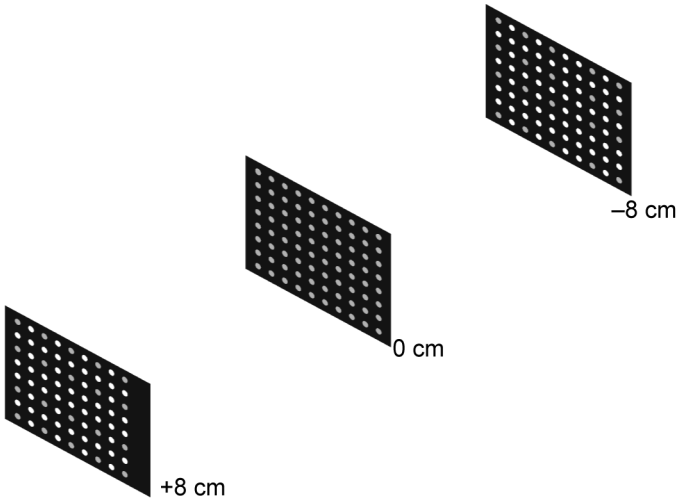

Figure 8.—Calibration grid pattern used for SOFBALL chamber.

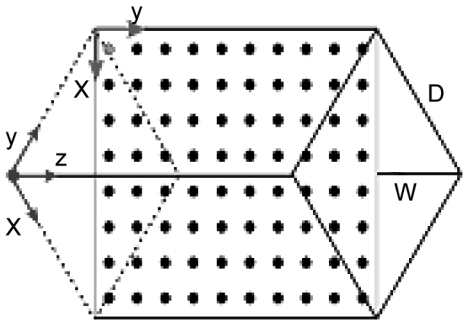

$$D^2 + D^2 = W^2$$
$$D = \sqrt{W^2/2}$$

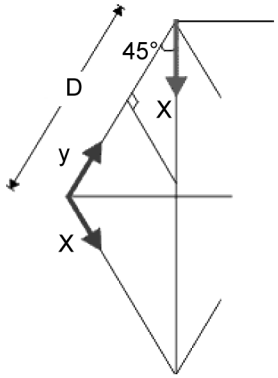

$$X = x\sin 45^o$$
$$Y = D - x\cos 45^o$$
$$Z = y$$

Figure 9.—Two to three-dimensional mapping of SOFBALL data.

Using the calibration coefficients from this set of calibration points as input when determining the 3–D corrected particle position for the test points gave an average, minimum and maximum distance from predicted particle position to actual particle position of

d_{avg} = 5.8137 pixels
d_{min} = 0.6494 pixels
d_{max} = 9.6089 pixels

Based on our calibration technique for the SOFBALL experiment, particle centroids can be determined with an average accuracy of 5.8 pixels (approximately 3.2 mm at the center plane of the chamber), which is our baseline error metric for the SOFBALL experimental chamber.

Results and Discussion

Our technique was used on over 3887 images, which covered 20 experiments. Each experiment consisted of up to 9 simultaneous flame balls over the entire experimental chamber. The goal was to accurately label and track each flame ball in 3–D. Since the complete data set is extremely large, we will present two different experiments with one experiment consisting of 3 flame balls and the other consisting of 9 flame balls.

We faced several challenges in analyzing the data for this experiment. The first challenge was to switch the calibration chamber from a vertical orientation to a horizontal orientation. This involved solving for a unique camera orientation specific to the experiment chamber orientation of the SOFBALL experiment (see figs. 6 and 9). Once the mathematics of the camera orientation were completed, the experimental data was processed by our standard SIV techniques and presented in graphic and table form. A second challenge was the morphology of the flameballs over time for each experiment. For certain experiments, flameballs were splitting, combining, disappearing or extremely faint. These conditions were automatically detected by our technique by way of inconsistent or missing data points. When this occurred, we had to manually verify the data for these conditions, which was time consuming but necessary for accuracy and completeness.

Figures 10 and 12 show the actual left and right images of a specific 3-flame ball and 9-flame ball experiment with the flame ball number superimposed on the image. In many of the images, the flame balls are exceeding dim and difficult to discern. Figures 11 and 13 show the experimental path of each flame ball for a typical data set.

Tables 1, 2, and 3 list the data generated from our SIV analysis of the image data shown in figures 10 and 11. Tables 4, 5, and 6 list the data generated from our SIV analysis of the image data shown in figures 12 and 13. Figures 14 and 15 list the 3–D scatter plot of the image data combining the left and right image data sets.

The results show that using SIV for flame balls data analysis can be helpful in identifying 3–D flame ball positions as well as for verifying numerical simulations of flame ball phenomena. In a typical SIV experiment, we use overlap decomposition to identify overlapping particles or objects. However, this experiment was unique in that the flame balls can actually shrink, grow, split and suddenly disappear from the field of view, which makes it extremely difficult to continuously track and label the flame balls. In cases where flame balls were not able to be continuous labeled, a new sequence was started. We did not have to use our traditional particle tracking scheme for the flame ball data, since it was designed to track and identify dozens of objects simultaneously. The flame balls were so few in this experiment that we manually tracked the flame balls and then stereo matched the particles directly.

It is now possible to provide accurate 3–D experimental data, which can provide input and verification for numerical models, which attempt to predict the behavior of flame ball phenomena in a SOFBALL experiment.

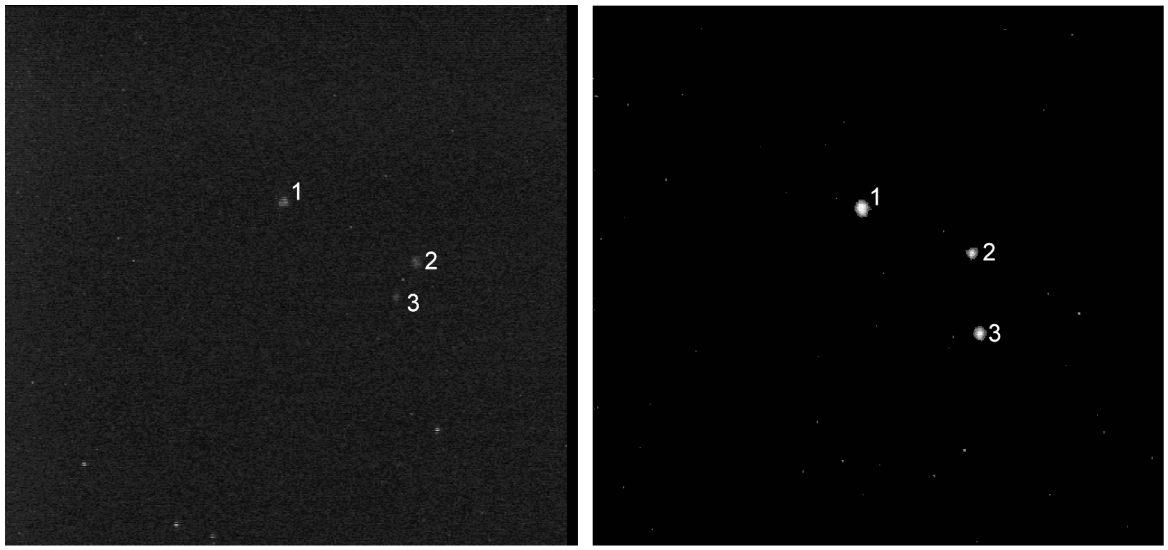

Left view Right view

Figure 10.—Three-flame ball example.

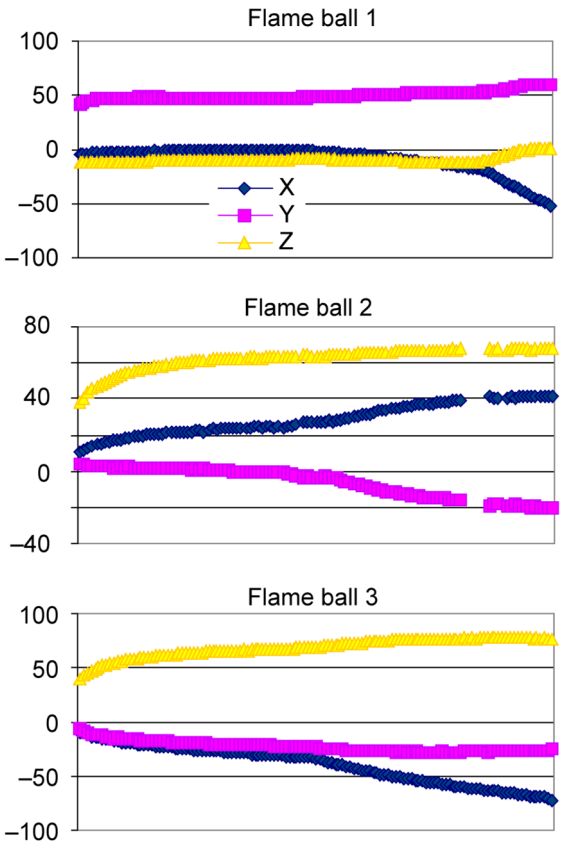

Figure 11.—Three-flame ball example listing the path of each flame ball.

TABLE 1.—3-FLAME BALL EXAMPLE—FLAME BALL 1

X [mm]	Y [mm]	Z [mm]
–4.7033	41.4913	–11.7937
–4.3665	43.2356	–12.1944
–3.9238	44.1074	–12.1982
–3.9211	45.118	–11.9903
–3.6528	45.6306	–12.1516
–3.6485	46.1343	–12.0986
–3.6985	46.6794	–11.8843
–3.4112	46.7731	–11.8015
–3.0084	46.7907	–11.921
–3.2457	47.0907	–11.7852
–2.9504	47.2316	–11.4077
–2.4959	47.0113	–11.7437
–3.1713	47.6094	–11.4194
–2.6009	47.2868	–11.4596
–2.4816	47.3744	–11.2666
–2.4662	47.4884	–11.3343
–2.3634	47.5362	–11.2105
–2.216	47.5058	–11.2915
–2.3393	47.7732	–11.09
–2.1016	47.6681	–11.2016
–2.3557	47.7375	–11.0654
–1.9636	47.6809	–10.9761
–2.3006	47.9002	–10.9846
–1.7298	47.5042	–10.8523
–2.3137	47.8998	–10.9131
–1.8939	47.6932	–10.7219
–1.792	47.621	–10.7598
–1.6854	47.5923	–10.562
–1.685	47.5962	–10.4677
–1.5374	47.6058	–10.3734
–1.2999	47.5048	–10.3904
–1.1896	47.3919	–10.3077
–1.7239	47.6355	–10.4411
–1.4456	47.4207	–10.3471
–1.551	47.5695	–10.3828
–1.0895	47.2755	–10.6151
–1.2727	47.473	–10.1563
–1.3034	47.5814	–10.4638
–1.419	47.5411	–10.328
–1.164	47.3998	–10.2621
–0.8765	47.1096	–10.0979
–1.0837	47.4067	–10.2034
–1.1674	47.4041	–10.1336
–1.2332	47.5213	–10.0069
–1.0441	47.375	–10.0409
–0.8603	47.2315	–9.9766
–1.1687	47.4101	–9.9748
–1.0199	47.3436	–9.7723
–0.9982	47.2722	–9.6796
–1.1647	47.3335	–9.9012
–0.7388	47.2008	–9.914
–0.9432	47.2365	–9.7174
–0.7348	47.0134	–9.7836
–0.7384	47.2489	–9.5141
–0.5956	46.8747	–9.3056
–0.9941	47.3899	–9.5807
–0.8303	47.205	–9.6169
–0.8281	47.2103	–9.4918
–0.6529	47.0624	–9.4841
–0.7353	47.1375	–9.4918
–0.6456	47.0688	–9.3627
–0.9555	47.2494	–9.2966
–0.7827	47.2502	–9.5997
–1.0336	47.3185	–9.4978
–0.4132	47.0848	–9.2425
–0.9201	47.4139	–9.0092
–0.9679	47.4522	–8.9445
–0.7585	47.4254	–8.9558
–1.2887	47.783	–9.1223
–1.003	47.6087	–8.8185
–1.3526	47.8193	–8.9809
–1.5201	48.0824	–8.9888
–2.08	48.404	–9.0584
–1.9296	48.256	–8.8041
–2.0716	48.323	–9.1128
–2.554	48.5698	–9.1049
–2.69	48.6056	–8.9003
–2.8048	48.7095	–9.2704
–3.2523	49.1147	–9.1344
–3.3523	49.181	–9.2546
–3.7645	49.3114	–9.4071
–3.7566	49.3089	–9.5403
–4.3734	49.4755	–9.4604
–4.2467	49.4401	–9.5614
–4.7212	49.49	–9.7043
–4.8552	49.6759	–9.8812
–5.4995	50.0334	–9.6602
–5.4332	49.7982	–9.9501
–5.8588	49.8944	–10.0768
–6.0885	50.0716	–10.2332
–6.5903	50.3949	–10.2195
–6.731	50.4616	–10.5191
–6.9934	50.4495	–10.2935
–7.2972	50.4696	–10.7218
–7.5264	50.7674	–10.6859
–8.4085	50.9595	–10.717
–8.5049	50.9902	–10.9816
–8.6032	50.8664	–10.9951
–9.1532	51.1177	–10.8863
–9.4622	51.3726	–11.0485
–10.0796	51.5342	–11.1106
–10.3748	51.5239	–11.099
–10.4771	51.6735	–11.1678
–10.5411	51.587	–11.2802
–11.2156	51.9097	–11.5053
–11.4353	51.8246	–11.3879
–11.6773	51.8121	–11.3306
–12.0712	52.0319	–11.466
–12.7635	52.2732	–11.5332
–12.7918	52.3478	–11.4962
–12.7631	51.9658	–11.5229
–13.4188	52.5188	–11.8125
–13.3418	52.249	–11.6966
–13.7487	52.1993	–11.5427
–13.7342	52.1232	–11.5071
–14.6867	52.4417	–11.75
–15.3053	52.6198	–11.4302
–15.6344	52.5749	–11.2503
–16.2648	52.7908	–11.2001
–16.8997	52.8938	–11.117
–17.4237	53.154	–11.0775
–17.6425	53.1488	–11.0337
–17.7999	53.1107	–11.035
–18.9948	53.2898	–10.278
–20.0246	53.0884	–10.1549
–21.4952	53.3491	–9.3063
–22.9772	53.7335	–8.8116
–24.4802	54.0272	–7.8811
–25.8691	53.9054	–7.2886
–27.6972	54.36	–6.7319
–29.5119	55.1561	–5.4046
–31.362	56.2646	–4.0053
–33.0647	56.7614	–3.1167
–34.7239	57.5161	–2.3442
–36.5777	58.1805	–1.7604
–38.1717	58.5827	–1.3224
–40.2471	59.0704	–0.9269
–41.9432	59.6323	–0.4462
–43.6615	60.1569	0.022
–44.4039	59.7734	0.1001
–45.9422	59.9971	0.4057
–47.0614	59.7813	0.6314
–49.3372	59.7125	0.6742
–50.8147	58.9212	0.6115
–53.1226	58.8868	0.8809

TABLE 2.—3-FLAME BALL EXAMPLE—FLAME BALL 2

X [mm]	Y [mm]	Z [mm]
10.5669	3.8053	37.8355
11.7556	3.7036	40.8668
12.8714	3.276	43.395
13.5921	3.0157	45.5584
14.6812	2.5527	46.9258
14.9178	2.8661	48.3263
15.707	2.6294	49.6447
16.261	2.4382	50.5183
17.0191	2.3105	51.6686
17.1767	2.16	52.1472
17.5502	2.5217	53.1581
18.1032	2.3387	54.1537
18.3027	2.5517	54.7519
19.0386	2.0487	55.2681
18.9488	2.3164	55.5443
19.4734	2.1245	56.4724
20.0671	1.8141	56.9803
20.0765	2.1324	57.2724
20.2828	1.9532	57.7311
20.1921	2.1551	58.2283
20.6076	2.0211	58.4623
21.3944	1.5669	59.2922
21.1614	1.8299	59.4066
21.3652	1.9245	59.6542
21.5939	1.6577	59.8976
22.0275	1.3664	60.028
21.8953	1.5588	60.229
22.1899	1.2695	60.8158
22.4803	1.2907	61.2226
22.6485	1.0213	61.3513
22.0648	1.5127	61.531
23.0329	0.8881	61.6259
23.346	0.6755	62.0376
23.0786	0.9784	62.1105
23.3153	0.5486	61.8821
23.776	0.4632	62.4637
23.9213	0.3538	62.5581
23.7298	0.1775	62.304
24.3062	–0.3055	62.5316
24.0312	0.0318	62.4174
24.089	–0.1935	62.8306
24.1244	–0.1457	62.9503
24.4959	–0.2479	63.0761
24.5611	–0.3704	62.8245
24.3395	–0.3831	62.7898
24.8318	–0.8272	63.1557
25.1268	–0.8024	63.5732
24.2456	–0.3015	62.9641
24.6987	–0.7146	63.1735
24.1324	–0.2291	62.9833
25.1038	–0.9609	63.7515
25.2511	–1.1509	63.7363
25.9282	–2.0894	63.2662
27.1972	–3.2506	64.0791
27.0779	–2.8945	64.141
27.4707	–3.1241	63.9345
27.1516	–3.2148	63.8506
27.2848	–3.3682	63.9791
26.9627	–3.1059	63.8948
27.7194	–3.6977	64.4542
27.7058	–3.6199	64.452
27.8428	–3.9273	64.5842
28.2395	–4.7095	64.5239
29.0478	–5.5135	64.6755
29.4987	–5.8465	65.118
29.9766	–6.7471	64.9579
30.9364	–7.506	65.2863
31.158	–7.7759	65.3934
31.7858	–8.3873	65.7876
31.7455	–8.8299	65.4392
32.443	–9.2435	65.694
33.3172	–10.2113	65.8975
33.6197	–10.4001	66.2073
33.8882	–11.0306	66.2068
34.4894	–11.2915	66.1474
34.9206	–11.8774	66.3995
35.159	–12.1905	66.2451
35.631	–12.2169	66.6973
35.5765	–12.4985	66.535
36.4937	–13.1927	66.5215
36.5829	–13.5914	66.8362
36.8565	–13.8239	66.7254
37.1823	–14.1759	66.8502
37.4606	–14.4895	66.9295
37.5765	–14.408	67.2145
37.7109	–14.7251	67.1951
37.8917	–14.9608	67.1076
37.9054	–14.9185	66.8822
38.4255	–15.4286	67.1504
38.9577	–15.8991	67.3446
38.772	–15.8226	67.2395
39.5402	–15.9671	67.5504
41.2096	–18.544	67.6046
40.7848	–18.5077	67.194
40.8986	–18.268	67.5192
40.8442	–18.548	67.3179
41.378	–18.9477	67.8576
40.4696	–18.2785	67.5664
41.5214	–19.2238	67.6097
41.7227	–19.3012	67.679
41.1104	–19.0309	67.6235
41.7106	–19.8992	67.3304
41.2115	–19.4699	67.5613
41.7337	–19.781	67.5259
41.6642	–19.8681	67.7434
41.3201	–19.8348	67.7671
41.6347	–20.1882	67.5845

Note: Blank row between data points represents incomplete track.

TABLE 3.—3-FLAME BALL EXAMPLE—FLAME BALL 3

X [mm]	Y [mm]	Z [mm]
–9.5148	–7.0174	38.845
–10.7623	–8.5491	42.476
–12.0128	–9.8434	45.194
–13.0736	–11.0167	47.4994
–13.7883	–11.9091	49.1608
–14.6043	–12.3997	50.766
–15.5665	–12.7964	51.7216
–16.3086	–12.9101	53.0675
–16.4728	–14.0719	53.8539
–16.9294	–14.7259	54.6901
–18.0201	–14.476	55.4697
–18.6211	–14.7319	55.9494
–18.8875	–15.5298	56.9037
–19.3195	–15.8123	57.2144
–20.0418	–15.6829	58.0537
–20.3553	–16.4452	58.6047
–20.748	–16.658	58.7229
–21.4728	–16.7188	59.4573
–21.4988	–17.2338	59.6736
–22.0112	–17.5337	59.9584
–22.3948	–17.6767	60.6251
–22.7378	–17.6186	61.013
–23.163	–18.1046	61.2431
–23.4324	–18.2366	61.7693
–23.5715	–18.6119	61.9614
–24.1715	–18.5834	62.1967
–24.3385	–18.8244	62.6746
–24.7782	–19.2655	62.5437
–25.1956	–19.4454	63.3578
–25.4025	–19.4545	63.6705
–25.8179	–19.7885	63.4478
–26.0481	–19.8834	63.8167
–26.3193	–19.9064	64.2116
–26.5405	–20.1825	64.5446
–26.7117	–20.2295	64.4433
–27.2245	–20.4628	64.3629
–27.0947	–20.5578	64.8691
–27.4109	–20.9308	65.0813
–27.758	–20.7973	65.3025
–28.2877	–20.7602	65.2261
–28.1503	–21.2452	65.8165
–28.5688	–21.1298	65.6367
–28.9499	–21.2771	65.7451
–29.1327	–21.2467	66.2216
–29.2941	–21.4818	65.9538
–29.5245	–21.5737	66.3831
–29.5388	–21.9561	66.6862
–30.1309	–21.4393	66.5843
–30.1229	–22.0025	66.6897
–30.4689	–21.9173	66.7494
–30.7196	–21.9727	66.8867
–30.6837	–22.0774	67.2092
–31.0846	–22.0744	67.3502
–31.1868	–22.2717	67.6081
–31.3585	–22.6632	67.4257
–31.3867	–22.7767	67.6701
–31.8327	–22.3898	67.4341
–31.7187	–22.837	68.1087
–32.2271	–22.6549	67.9792
–32.3245	–22.9648	68.0071
–32.7422	–22.6519	68.2224
–32.6614	–22.8347	68.6138
–33.6553	–23.6355	68.9044
–34.787	–23.9538	69.3175
–35.9372	–24.2016	70.1772
–36.704	–24.368	70.5754
–37.6745	–24.8728	70.9123
–38.7025	–24.9148	71.2658
–39.7102	–25.1963	71.4201
–40.3593	–25.5876	71.886
–41.2159	–26.0497	71.9604
–42.1661	–26.054	72.0511
–42.9967	–26.2518	72.0933
–43.7512	–26.5082	72.3285
–44.6351	–26.9364	72.4313
–45.0706	–27.0007	73.6838
–45.8016	–26.8298	73.9641
–46.5333	–26.929	74.2796
–47.2029	–26.9098	74.4647
–47.8834	–27.0084	74.6664
–48.8319	–26.9012	74.8444
–49.3488	–26.9848	74.984
–49.8892	–27.3078	75.2867
–50.6368	–27.544	75.2794
–51.2484	–27.4355	75.5806
–51.9356	–27.4297	75.5193
–52.4039	–27.7534	75.646
–53.0141	–27.5707	75.8031
–53.7449	–27.5144	76.0774
–54.0868	–27.907	76.2194
–54.5451	–27.7109	76.2809
–55.2001	–27.6658	76.1712
–55.7605	–27.8047	76.2429
–56.3529	–27.7012	76.3637
–56.6912	–28.0563	76.5113
–57.447	–27.4839	76.6314
–57.8922	–27.6526	76.6861
–58.328	–27.5249	76.9356
–59.048	–27.5381	76.6894
–59.3254	–27.6377	76.9353
–59.8454	–27.5288	77.0107
–60.3325	–27.3717	77.1327
–60.699	–27.5065	76.9636
–61.1596	–27.4649	77.168
–61.6283	–27.4444	77.0581
–61.9547	–27.4609	77.399
–62.4771	–27.4514	77.2203
–62.8045	–27.7464	77.1002
–63.3535	–27.1769	77.2922
–63.6592	–27.178	77.2086
–64.0217	–27.3442	77.2483
–64.5038	–26.9385	77.3114
–64.9619	–26.9654	77.1383
–65.2186	–27.1115	77.2899
–65.5221	–27.1075	77.2726
–66.3115	–26.6451	77.4417
–66.8549	–26.3358	77.3892
–67.2153	–26.776	77.1615
–67.8944	–26.2672	77.1706
–68.4761	–26.1398	77.002
–68.4916	–26.2215	77.0781
–69.1061	–26.1897	76.8332
–68.882	–26.6081	77.0902
–70.3335	–25.8715	76.8753
–71.7397	–25.2139	77.015

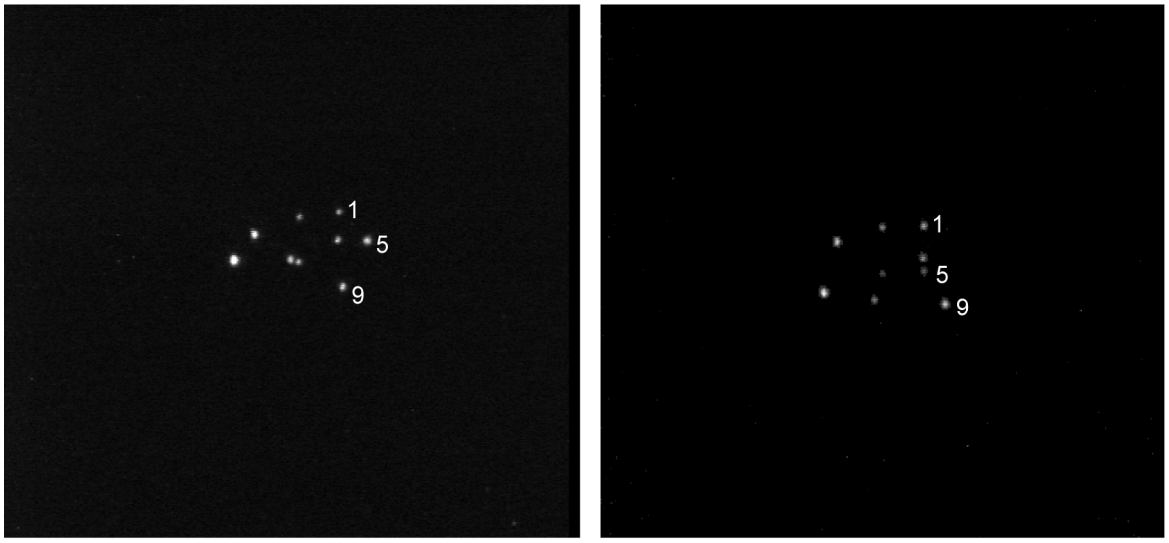

Left view Right view

Figure 12.—Nine-flame ball example.

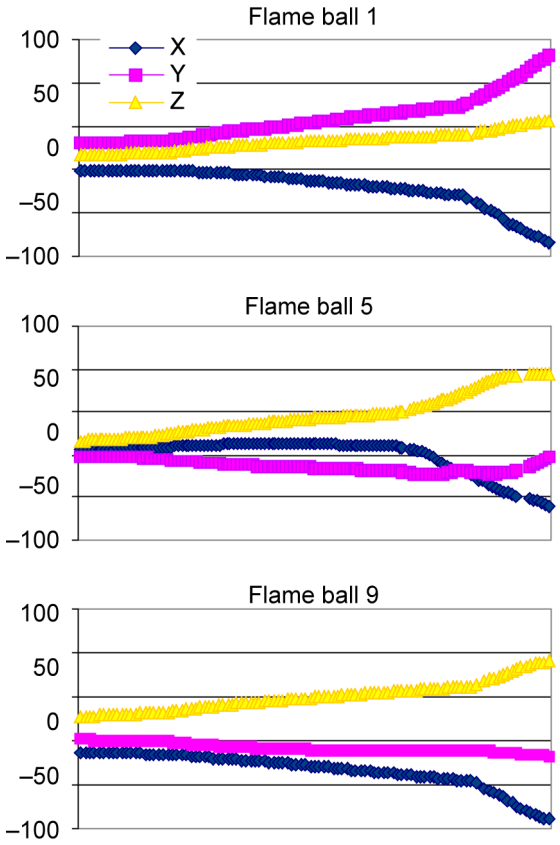

Figure 13.—Nine-flame ball example listing the path of flame balls 1, 5, and 9.

TABLE 4.—9-FLAME BALL EXAMPLE—FLAME BALL 1

X [mm]	Y [mm]	Z [mm]	X [mm]	Y [mm]	Z [mm]
–2.2003	29.951	16.4428	–12.6645	54.5856	32.7534
–2.0774	30.1957	16.6708	–13.3496	55.1863	32.9997
–2.1281	30.5788	16.597	–13.8148	55.9935	33.2453
–1.9712	30.5967	16.8996	–14.2662	56.4905	33.5267
–1.9846	30.7595	17.1641	–14.8309	57.0599	33.8113
–2.078	30.9132	17.3251	–15.2179	57.676	34.0678
–1.9839	31.1199	17.5256	–15.9425	58.4299	34.1706
–1.9588	31.2415	17.6572	–16.383	58.9675	34.4653
–1.9553	31.5182	17.8826	–16.8886	59.7352	34.7018
–1.9522	31.5213	17.9511	–17.2744	60.353	34.9607
–1.9459	31.8011	18.245	–17.8555	60.8046	35.1794
–1.9053	32.1187	18.2799	–18.4624	61.4095	35.2713
–1.9061	32.1186	18.3117	–18.8267	61.842	35.7485
–1.7857	32.3648	18.6375	–19.4436	62.5613	35.7817
–1.682	32.4925	18.7417	–19.8969	63.3289	35.9349
–1.5742	32.4542	18.734	–20.5078	63.7099	36.248
–1.7149	32.7265	18.932	–20.8603	64.4073	36.4823
–1.7599	32.8503	19.2318	–21.4956	64.7812	36.6711
–1.5357	32.8619	19.234	–21.8293	65.3657	36.879
–1.9313	33.3571	19.5251	–22.3188	65.8649	37.1512
–1.792	34.0839	20.2786	–22.9537	66.4715	37.2777
–1.7233	34.7271	21.0283	–23.6306	67.208	37.6162
–1.8692	35.7435	21.6304	–24.2198	67.7807	37.8093
–1.8698	36.3051	22.3465	–24.7206	68.247	38.101
–2.3475	36.9917	22.8191	–25.2746	68.86	38.2081
–2.378	37.7066	23.4951	–25.734	69.3981	38.3243
–2.8158	38.5528	24.0886	–26.2033	69.8226	38.5692
–2.8464	39.1821	24.4618	–26.885	70.5625	38.8095
–3.1441	39.8415	25.029	–27.3594	71.1045	39.0662
–3.1828	40.555	25.5706	–27.8281	71.6154	39.27
–3.6504	41.4726	25.8869	–28.3259	71.9992	39.4501
–4.0372	42.1267	26.442	–28.7937	72.4296	39.7279
–4.2226	42.7491	26.7459	–29.5919	73.1305	39.9789
–4.7646	43.5058	27.1101	–29.933	73.7601	40.1841
–5.0676	43.9697	27.5203	–32.9008	76.3166	40.8578
–5.3114	44.6294	27.9093	–38.2896	81.5354	42.9191
–5.7129	45.2778	28.1892	–41.1108	84.2739	43.7116
–6.1732	45.8481	28.571	–44.1639	86.8067	44.4686
–6.1834	45.7421	29.0409	–46.8293	89.4734	45.5081
–6.7295	46.1846	29.1324	–49.9553	92.3463	46.3616
–6.9841	46.6423	29.2573	–52.6618	94.8577	47.1544
–7.4306	47.3313	29.6006	–57.2232	98.3504	48.0644
–7.93	48.0596	30.0653	–62.2202	101.8027	49.1799
–8.8481	48.9155	30.2358	–63.906	103.4469	50.9128
–9.0372	49.6523	30.3266	–66.2535	106.0944	51.2008
–9.1645	50.0062	30.6833	–68.9406	109.2235	51.9175
–9.7301	50.6503	30.9796	–71.704	112.8583	52.839
–10.2591	51.4553	31.3624	–75.2743	117.8704	53.731
–10.7675	52.1824	31.6885	–77.7529	121.2889	53.4885
–11.2887	52.7937	32.0852	–77.9566	124.0232	54.8715
–11.7566	53.3636	32.264	–80.6406	127.263	55.8071
–12.2518	53.9309	32.4482	–84.4242	131.3436	56.7102

TABLE 5.—9-FLAME BALL EXAMPLE—FLAME BALL 5

X [mm]	Y [mm]	Z [mm]
6.8558	–2.3052	16.8634
6.7988	–2.5759	16.8946
7.1456	–2.5826	17.2402
7.0941	–2.6949	17.5047
7.1942	–3.0306	17.5705
7.1399	–3.0655	17.9055
7.5016	–3.0724	18.1781
7.523	–3.2608	18.2485
7.4623	–3.4496	18.5789
7.5824	–3.4763	18.7139
7.8267	–3.3739	19.1201
7.7242	–3.6885	19.082
7.707	–3.4162	19.3113
8.0293	–3.7349	19.4979
8.0737	–3.7629	19.8254
8.1509	–3.7568	19.8636
8.258	–3.9345	20.1651
8.3268	–4.0788	20.3664
8.4903	–3.9087	20.6436
8.4578	–4.2137	20.8467
8.7816	–4.6731	21.6889
9.1645	–5.2845	22.6613
9.4266	–5.5225	23.3401
9.6288	–6.0199	24.249
9.9095	–6.4449	25.0451
10.1302	–6.725	25.6637
10.3148	–7.0437	26.3492
10.6615	–7.2814	26.9031
10.9044	–7.4091	27.5501
11.1007	–7.7266	28.3052
11.3131	–8.1614	28.9023
11.3763	–8.4531	29.4558
11.5108	–8.7413	30.0829
11.3942	–8.9293	30.555
11.5557	–9.3321	31.1208
12.0516	–9.5262	31.6515
12.151	–9.7823	32.0739
12.2258	–10.0752	32.6286
12.6885	–11.1149	33.1976
12.6366	–11.8426	33.3917
12.6689	–12.1043	33.7043
12.6704	–12.251	34.185
12.6891	–12.3592	34.7077
12.7129	–12.3534	35.0476
12.7438	–12.4633	35.3619
12.9835	–12.6768	35.7222
12.9227	–13.1345	36.2503
12.9368	–13.2072	36.5242
12.8736	–13.2047	37.0348
12.9203	–13.3507	37.5992
12.9094	–13.6939	37.8863
12.9959	–13.8398	38.2375
13.1144	–14.1373	38.671
12.9118	–14.3741	39.0111
12.8512	–14.4878	39.4962
12.9098	–14.6378	39.5743
12.8095	–14.9064	40.064
12.7909	–15.0581	40.3783
12.6583	–15.099	40.7866
12.6393	–15.3647	41.1432
12.668	–15.3615	41.4878
12.7743	–15.4279	41.9245
12.6797	–15.7736	42.3779
12.4898	–15.855	42.749
12.4164	–16.0829	43.103
12.2816	–16.1234	43.5107
12.3614	–16.4223	43.6707
12.2962	–16.5368	44.0166
12.3435	–16.5709	44.4376
12.0574	–16.768	44.6679
11.9853	–16.9595	45.0484
11.9972	–17.1058	45.2348
11.7964	–17.2623	45.708
11.6245	–17.4567	45.9418
11.6755	–17.6047	46.2295
11.4305	–17.9146	46.4945
11.5046	–17.8293	46.9216
11.2935	–18.0654	46.9755
11.1335	–18.2151	47.2139
11.0446	–18.2484	47.4902
10.8233	–18.2916	47.8166
10.8415	–18.6246	48.041
10.7501	–18.8923	48.3495
10.667	–19.035	48.7344
10.1157	–19.3824	49.4462
9.8694	–19.7368	49.6286
8.9659	–20.5039	50.7465
6.9264	–21.9316	53.4015
5.8029	–22.6593	54.419
4.4735	–23.3451	55.6705
3.1153	–23.8631	56.826
1.7124	–23.9413	58.1176
0.0112	–24.2276	59.2504
–3.5157	–24.3284	60.3759
–8.3349	–24.2196	61.4391
–10.1506	–24.182	63.4633
–11.9619	–23.2377	64.0696
–14.0253	–21.8892	65.4563
–16.4157	–21.095	67.3837
–18.4792	–19.4624	69.5509
–19.7483	–19.2272	70.3575
–19.2919	–18.6457	72.9375
–21.2698	–19.636	74.7126
–24.4121	–20.256	76.5814
–26.9205	–20.8865	78.2856
–29.4511	–21.0991	80.4868
–31.5365	–21.7343	82.5495
–33.6833	–22.1107	84.3316
–35.9591	–22.5964	85.9998
–37.0992	–22.3904	87.4387
–39.756	–22.8309	88.8178
–41.7474	–22.3877	90.0496
–43.5465	–22.1615	91.1084
–45.2988	–21.7018	91.8939
–46.6454	–20.5826	92.3481
–48.0607	–19.6285	92.8223
–52.151	–13.5482	93.8659
–52.982	–11.7651	94.0355
–53.9152	–9.2521	94.0212
–54.9752	–7.0088	94.31
–58.5181	–4.6251	95.0106
–59.9607	–1.8127	95.2823

TABLE 6.—9-FLAME BALL EXAMPLE—FLAME BALL 9

X [mm]	Y [mm]	Z [mm]	X [mm]	Y [mm]	Z [mm]
–13.8952	1.3663	27.2773	–28.916	–10.37	49.1181
–13.8104	1.3752	27.4722	–29.464	–10.5548	49.6073
–13.9832	1.2186	27.8802	–29.7827	–10.4122	49.9487
–14.202	1.052	28.0558	–30.3583	–10.6399	50.3998
–13.9884	0.9211	28.5156	–30.9117	–10.6677	50.83
–14.3571	0.7471	28.8099	–31.3436	–10.7317	51.1167
–14.5484	0.6991	28.9584	–31.8866	–10.835	51.6368
–14.349	0.757	29.2893	–32.523	–10.7539	51.9651
–14.584	0.5168	29.6562	–33.0184	–10.6227	52.3432
–14.4512	0.3751	29.8245	–33.5034	–10.6088	52.6866
–14.6429	0.0946	29.9998	–33.6512	–10.6766	53.2859
–14.5621	0.1043	30.2282	–34.345	–10.7597	53.5666
–14.7237	0.0226	30.5063	–34.8336	–10.9799	54.022
–14.7279	–0.2029	30.8543	–35.3309	–11.0488	54.2653
–14.8225	–0.284	30.9136	–35.9007	–10.9199	54.6313
–14.9233	–0.2469	31.194	–36.4956	–11.0303	55.014
–14.9055	–0.3216	31.3511	–36.8111	–11.0818	55.3734
–15.1184	–0.3692	31.4996	–37.3007	–11.1366	55.8618
–15.1104	–0.3263	31.8467	–37.8072	–11.2387	56.2855
–15.1609	–0.5175	32.0973	–38.3678	–11.4285	56.5732
–15.5493	–1.4873	33.1767	–38.8888	–11.4559	56.8736
–15.986	–1.8079	34.1277	–39.4318	–11.3184	57.3326
–16.4192	–2.5559	34.9433	–39.9821	–11.4994	57.8043
–16.7904	–2.8762	35.6732	–40.4815	–11.2371	58.243
–17.4663	–3.4522	36.3064	–40.9339	–11.4587	58.5405
–17.8322	–3.9242	37.2205	–41.3893	–11.5543	58.9661
–18.2972	–4.4081	37.8073	–41.9783	–11.4603	59.3526
–18.3847	–4.7086	38.4951	–42.5427	–11.6107	59.6376
–18.9226	–5.1657	38.9412	–43.0605	–11.6328	59.9954
–19.4065	–5.3779	39.6233	–43.4414	–11.4732	60.5354
–19.7646	–5.8932	40.2137	–43.9217	–11.7008	60.7623
–20.1218	–6.061	40.8096	–44.4226	–11.921	61.1717
–20.6272	–6.3988	41.2572	–45.0123	–11.9795	61.6998
–20.9518	–6.7976	41.7236	–45.4037	–11.9899	62.0715
–21.3595	–6.9745	42.1818	–46.0295	–11.9382	62.4158
–21.7251	–7.1468	42.583	–48.5988	–12.0482	63.9749
–22.2517	–7.4497	42.992	–53.6245	–12.4881	67.8888
–22.6339	–7.7724	43.608	–56.2204	–12.4967	69.5827
–22.8642	–8.8621	44.1544	–58.9238	–12.8301	71.4973
–23.3365	–9.3587	44.309	–61.6143	–13.1235	73.4469
–23.5028	–9.5952	44.6318	–64.3507	–13.4741	75.2779
–24.1186	–9.5974	45.0631	–67.1189	–13.7087	77.1359
–24.7539	–9.6351	45.4631	–71.0258	–13.8732	79.0677
–25.2417	–9.7052	45.8431	–75.7241	–14.582	81.1186
–25.6852	–9.7678	46.2615	–77.1892	–16.452	83.5973
–25.9937	–9.8208	46.6327	–79.2894	–16.4465	84.5218
–26.4436	–10.0386	47.1064	–81.3811	–16.5532	86.1278
–26.8395	–9.978	47.5956	–83.6177	–16.7466	87.8303
–27.3859	–9.9307	47.972	–86.4106	–16.3455	89.3807
–28.0887	–10.1279	48.4142	–88.9347	–16.4711	89.5668
–28.4961	–10.3048	48.8281	–89.0446	–17.2232	91.8084

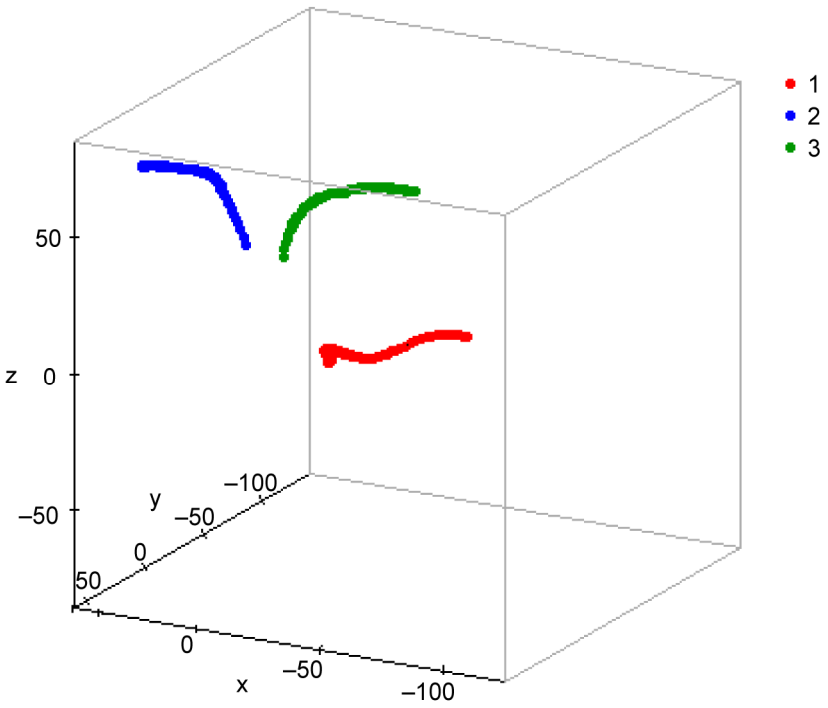

Figure 14.—Three-D scatter plot of three-flame ball example.

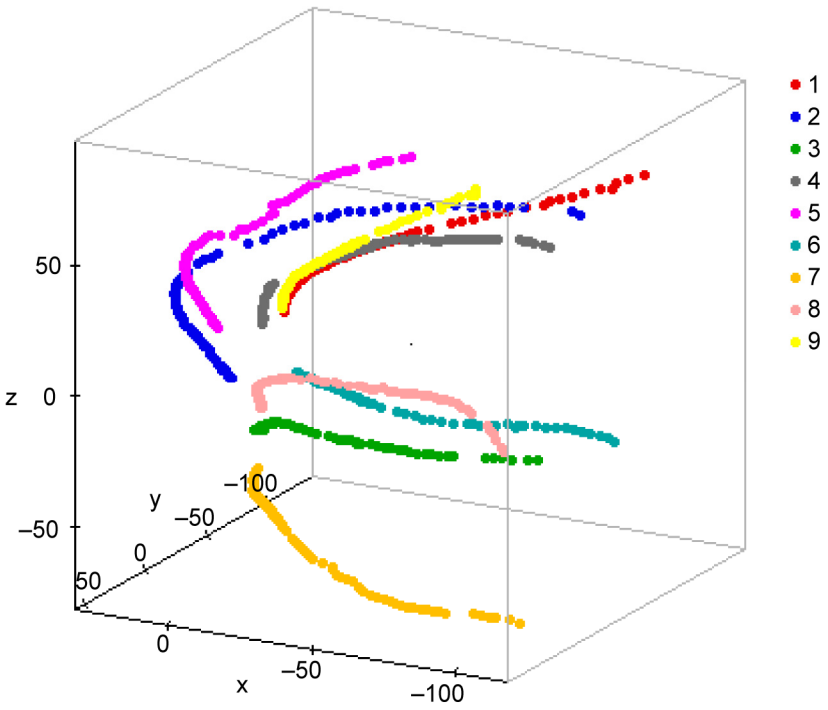

Figure 15.—Three-D scatter plot of nine-flame ball example.

Summary

An SIV technique for analyzing the Structure of Flame Balls At Low Lewis-number (SOFBALL) experiment studying flame balls has been develop and described. The goal was to develop a technique to accurately calculate the 3–D position of a flame ball(s) during an experiment, which can be used as a direct comparison of numerical simulations. This technique is applicable to any experiment that involves tiny, stable, stationary or spherically-symmetrical combustion phenomena occurring in a gas mixture experiment.

References

Bethea, M.D., Lock, J.A., Merat, F.L., and Crouser, P.D., (1997), Three-Dimensional Camera Calibration Technique for Stereo Imaging Velocimetry Experiments. Optical Engineering vol. 36, num. 12, pp. 3445–3454.

Bethea, M.D., (1996), High Precision Algorithms for Stereo Imaging Velocimetry. Ph.D. Dissertation, Department of Computer Engineering and Science, Case Western Reserve University, (1996).

Crouser, P.D., Bethea, M.D., and Merat, F.L., (1995), An Evolutionary, Neural Net Model for Globally-Optimized Particle Tracking. Presented at the Ohio Aerospace Institute Conference on Neural Networks.

McDowell, M. and Gray, E., (2004), Stereo Imaging Velocimetry. NASA Technical Publication (NASA/TP—2004-213112).

McDowell, M., (2004), An Integrated Centroid Finding and Particle Overlap Decomposition Algorithm for Stereo Imaging Velocimetry. NASA Technical Memorandum (NASA/TM—2004-213365).

McDowell, M., (2003), Stereo Imaging Velocimetry System and Method. US Patent #6,603,535, 2003.

McDowell, M. and Glasgow, T., (1999), U.S. Patent #05905568, “Stereo Imaging Velocimetry.”

Miller, B.B., Meyer, M.B., Meyer, and Bethea, M.D., (1994), Stereo Imaging Velocimetry for Microgravity Applications. International Symposium on Space Optics, Garmish-Partenkirchen, FRG.

Trigui, N., Guezennec, Y., Brodkey, R., and Kent, C., (1992), Fully Automated Three-Dimensional Particle Image Velocimetry System Applied to Engine Fluid Mechanics Research. Proc. of Optical Methods and Data Proc. in Heat and Fluid Flow, London, 1992.

REPORT DOCUMENTATION PAGE	Form Approved OMB No. 0704-0188

1. REPORT DATE *(DD-MM-YYYY)*	2. REPORT TYPE	3. DATES COVERED *(From - To)*
01-04-2008	Technical Memorandum	

4. TITLE AND SUBTITLE
A Stereo Imaging Velocimetry Technique for Analyzing Structure of Flame Balls at Low Lewis-Number (SOFBALL) Data

5a. CONTRACT NUMBER

5b. GRANT NUMBER

5c. PROGRAM ELEMENT NUMBER

6. AUTHOR(S)
McDowell, Mark; Gray, Elizabeth

5d. PROJECT NUMBER

5e. TASK NUMBER

5f. WORK UNIT NUMBER
WBS 561581.02.08.03.16.02

7. PERFORMING ORGANIZATION NAME(S) AND ADDRESS(ES)
National Aeronautics and Space Administration
John H. Glenn Research Center at Lewis Field
Cleveland, Ohio 44135-3191

8. PERFORMING ORGANIZATION REPORT NUMBER
E-16404

9. SPONSORING/MONITORING AGENCY NAME(S) AND ADDRESS(ES)
National Aeronautics and Space Administration
Washington, DC 20546-0001

10. SPONSORING/MONITORS ACRONYM(S)
NASA

11. SPONSORING/MONITORING REPORT NUMBER
NASA/TM-2008-215162

12. DISTRIBUTION/AVAILABILITY STATEMENT
Unclassified-Unlimited
Subject Categories: 23, 07, and 35
Available electronically at http://gltrs.grc.nasa.gov
This publication is available from the NASA Center for AeroSpace Information, 301-621-0390

13. SUPPLEMENTARY NOTES

14. ABSTRACT
Stereo Imaging Velocimetry (SIV) is a NASA Glenn Research Center (GRC) developed fluid physics technique for measuring three-dimensional (3-D) velocities in any optically transparent fluid that can be seeded with tracer particles. SIV provides a means to measure 3-D fluid velocities quantitatively and qualitatively at many points. This technique provides full-field 3-D analysis of any optically clear fluid or gas experiment using standard off-the-shelf CCD cameras to provide accurate and reproducible 3-D velocity profiles for experiments that require 3-D analysis. A flame ball is a steady flame in a premixed combustible atmosphere which, due to the transport properties (low Lewis-number) of the mixture, does not propagate but is instead supplied by diffusive transport of the reactants, forming a premixed flame. This flame geometry presents a unique environment for testing combustion theory. We present our analysis of flame ball phenomena utilizing SIV technology in order to accurately calculate the 3-D position of a flame ball(s) during an experiment, which can be used as a direct comparison of numerical simulations.

15. SUBJECT TERMS
Computer vision; Combustion chamber; Image analysis; Pattern recognition

16. SECURITY CLASSIFICATION OF:			17. LIMITATION OF ABSTRACT	18. NUMBER OF PAGES	19a. NAME OF RESPONSIBLE PERSON
a. REPORT	b. ABSTRACT	c. THIS PAGE			STI Help Desk (email:help@sti.nasa.gov)
U	U	U	UU	24	19b. TELEPHONE NUMBER *(include area code)* 301-621-0390